



## **SYNTHESIS AND ELECTRICAL CHARACTERISATION OF BISMUTH DOPED YTTRIUM OXIDE**

**G. BHAVANI<sup>a</sup>, S. GANESAN<sup>b</sup>, S. SELVASEKARAPANDIAN<sup>c</sup>,  
S. MONISHA<sup>c</sup> and M. PREMALATHA<sup>c</sup>**

<sup>a</sup>Department of Physics, Jansons Institute of Technology, COIMBATORE (T.N.) INDIA

<sup>b</sup>Sri Shakthi Institute of Engineering and Technology, COIMBATORE (T.N.) INDIA

<sup>c</sup>Materials Research Center, COIMBATORE (T.N.) INDIA

### **ABSTRACT**

Nanosized metal oxides, in a variety of morphologies (such as particles, spheres, rods, and sheets), have attracted a great deal of attention in wide areas of research and technology. Yttrium oxide, as an important member among rare-earth compounds, has been actively studied in the recent years. It is one of the most promising elements to act as gate materials for MOSFETs instead of SiO<sub>2</sub>. Hence Yttrium oxide is selected as the host lattice for the study and the simple, cost effective precipitation methods are chosen as synthesis methods. Pure yttrium oxide and bismuth doped yttrium oxide samples of three doping concentration are prepared by sol-gel method. FTIR studies confirm the presence of functional groups in the samples. XRD studies show amorphous nature with broad hump for pure yttrium oxide samples and better crystallinity is observed for bismuth doped yttrium oxide samples. From the electrical studies it has been observed that the maximum conductivity achieved was for pure sample. Further, it is also observed that the pure sample has the highest dielectric constant values than the bismuth doped yttrium oxide samples. It may be due to the introduction of holes in the host yttrium oxide. Dielectric studies show that loss tangent is found to be less at high frequency.

**Key words:** Nanosized metal oxide, Bismuth doped Yttrium oxide.

### **INTRODUCTION**

Y<sub>2</sub>O<sub>3</sub> possesses some unique properties. Y<sub>2</sub>O<sub>3</sub> has a wide energy band gap, high electrical resistivity range (10<sup>11</sup>-10<sup>12</sup>ohm/m), dielectric permittivity (11-15), and electric strength (10<sup>8</sup>-10<sup>9</sup> Vm<sup>-1</sup>); it also shows low dielectric losses (0.01-0.03) and good transparency in a wide spectral range with little light diffusion<sup>1-4</sup>. Due to these properties, Y<sub>2</sub>O<sub>3</sub> is a prospective material for antireflection and protective coatings, interference mirrors

---

\* Author for correspondence; E-mail: bhavaneeg@gmail.com; Ph.: +91-8122062621

and for manufacturing passive components and dielectric layers in multilevel integrated circuits<sup>2</sup>. Much attention, therefore, has been paid to  $Y_2O_3$  nanomaterials also for memory devices owing to their electrical characteristics and potential applications<sup>5</sup>. The structural and electrical properties of stoichiometric  $Y_2O_3$  have been studied theoretically and the effect of neutral oxygen vacancies on the electronic structure of  $Y_2O_3$  was investigated earlier<sup>6-9</sup>. Hence an attempt is made in this paper to study the influence of bismuth dopant and the doping concentration on the structural and electrical properties of yttrium oxide, as host lattice.

## EXPERIMENTAL

Pure and bismuth doped yttrium oxide samples are prepared by sol-gel method. In this method, pure yttrium oxide A pure, and the bismuth doped yttrium oxide powders AB1, AB2, AB3 having three different dopant concentration have been prepared using the precursor, Yttrium Nitrate hexahydrate ( $Y(NO_3)_3 \cdot 6H_2O$ ) and Bismuth nitrate as dopant precursor. 1 g of Yttrium nitrate hexahydrate was dissolved in 10 ml of distilled water and stirred for long time to dissolve the salt completely followed by ammonium hydroxide added in drops to get clear solution of pure sample, A Pure. To prepare AB1, AB2 and AB3, 0.0025 g, 0.005 g and 0.01 g of bismuth nitrate respectively was added to the solution followed by the addition of 50 mL of ammonium hydroxide. Continuous stirring lead to precipitate and the precipitate was left for 15 hrs to settle. Then the obtained precipitate was washed with water and dried in an oven at 373 K for 3 hrs. After drying, the powder was finely ground. Calcination is done by heating the sample at 623 K in a muffle furnace for 15 hrs to obtain pure yttrium oxide and bismuth doped yttrium oxide powder<sup>10</sup>.

Jasco-FTIR 4100/japan make is used to take FTIR studies in the range of 500-4000  $cm^{-1}$ . The powder XRD study is carried out using a Shimadzu XRD 6000 X-ray diffractometer using  $CuK\alpha$  radiation. Impedance analysis is done by HIOKI 3532 LCR impedance analyser interfaced with a computer in the frequency range of 42 Hz to 1 MHz at room temperature.

## RESULTS AND DISCUSSION

### FTIR

Fig. 1 shows FTIR spectra of pure and bismuth doped yttrium oxide samples of three different dopant concentrations prepared by sol-gel method. Infrared studies were carried out in order to ascertain the purity and nature of the samples. The band centred within the range 560-700  $cm^{-1}$  is attributed to Y-O stretching mode of  $Y_2O_3$  structure<sup>11</sup>. The absorption band

of O-H stretching vibrations appears within the range  $3300 - 3400 \text{ cm}^{-1}$ . The band within the range  $740 - 990 \text{ cm}^{-1}$  corresponds to Bi-O stretching. The band around  $1400 \text{ cm}^{-1}$  is attributed due O-H bending<sup>12</sup> and it was observed that there is both broadening of band and shift in band with respect to dopant concentration. Although efforts were made to limit sample exposure to humidity, it is likely that samples adsorb traces of moisture during transfer from the sample box to the FTIR sample chamber, resulting in some hydrolysis<sup>13</sup>. Both sharpening and broadening of band occurs around  $740 - 990 \text{ cm}^{-1}$  with increasing concentration of dopant, shows the effect of bismuth concentration in the structure.

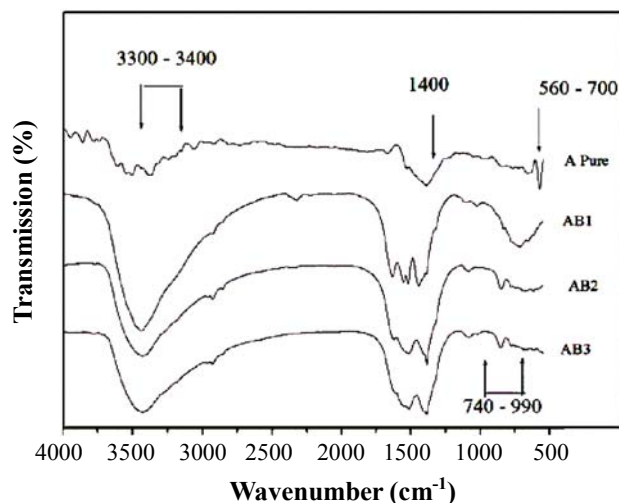


**Fig. 1: FTIR spectra of pure and bismuth doped yttrium oxide samples**

### Structural studies

XRD pattern of pure yttrium oxide and bismuth doped yttrium oxide samples of three different dopant concentrations prepared by sol-gel method is shown in Fig. 2. Average crystallite sizes of synthesized particles estimated to be 13 nm from the well-defined known Debye-Scherrer's equation [14]. It was observed that the structure of the pure sample shows amorphous nature with hump around  $30^\circ$  (222) plane and emerging peaks around  $27^\circ$  and  $48.5^\circ$ . And it has been observed that the doped samples show peaks characteristic of Monoclinic (JCPDS 391063) structure of yttrium oxide, which is enhanced due to doping and mixed with amorphous nature. The emerging peaks show that the samples are started to crystallize. It was also observed that the crystallinity increases with doping concentration but with higher doping concentration (1 weight percentage) the crystallinity decreases which may be due to the structural deformation produced by the dopant in the host lattice.

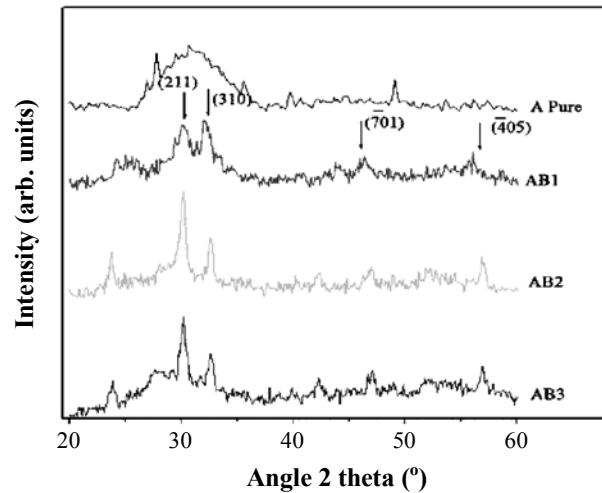


**Fig. 2: XRD pattern of pure yttrium oxide and bismuth doped yttrium oxide**

It has been found that the doped Bi ions had little influence on the host  $Y_2O_3$  structure. Also it was observed that the bismuth doping increased the lattice parameters of the samples, due to the fact that the ionic radius of  $Y^{3+}$  (0.092 nm) are slightly lower than  $Bi^{3+}$  (0.096 nm). Thus, the shifting of peak position to lower angle with increase in dopant concentration indicates the expansion of lattice parameters<sup>15</sup>.  $Bi^{3+}$  ions were expected to occupy the  $Y^{3+}$  sites in this phosphor.

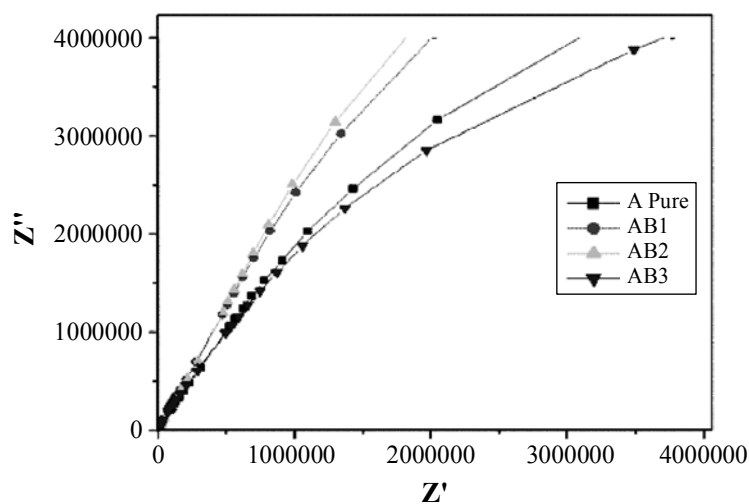
### Electrical studies

Fig. 3 shows complex impedance spectrum (Nyquist plots, i.e.  $Z''$  versus  $Z'$  also called Cole-Cole plots) of the pure yttrium oxide and bismuth doped yttrium oxide samples of three different dopant concentration. It shows only single semi-circular arcs whose radii gradually decrease with increase in doping concentration at room temperature. The intercepts of each semi-circular arc with the real axis ( $Z'$ ) give us the bulk resistance of the material and is extracted from the impedance plots using EQ software developed by Boukamp<sup>16,17</sup>. The high frequency arc can be represented by a parallel combination of a constant phase element (due to the immobile ions that became polarized in an alternating field) and a resistor (due to the mobile ion in the host matrix). The value of  $R_b$  is observed to decrease with increasing dopant concentration.

Conductivity of the bismuth doped yttrium oxide samples containing 0, 0.25, 0.5 and 1 weight percentage of yttrium precursor as dopant concentration were determined by the formula,

$$\sigma = l/R_b A \quad \dots(1)$$

Where  $l$  is the thickness of the pellet,  $A$  is its area and  $R_b$  is the bulk resistance. Initially, upon the addition of bismuth from 0.25 to 0.5 weight percentage, the conductivity of the yttrium oxide samples is observed to gradually increase slightly. The increase in conductivity can be attributed to the increase in mobile ion concentration. However, the conductivity is observed to decrease at the bismuth concentration of 1 weight percentage. The decrease in conductivity could be assigned to the dominating role of ion association over free ion formation, which decreases the number of charge carriers for conduction<sup>18</sup>.



**Fig. 3: The complex impedance plots of pure yttrium oxide and bismuth doped yttrium oxide samples**

Pure sample has conductivity maximum value as  $3.5 \times 10^{-7} \text{ Scm}^{-1}$  and it decreases with doping. The dielectric constants have frequency dependence, especially, at the low-frequencies, which is called the low frequency dielectric dispersion. All the samples show a strong frequency dispersion of permittivity in the lower frequency region, whereas it shows a nearly frequency independent behaviour at higher frequency region irrespective of dopant concentration. The decrease of dielectric constant with increase in frequency may be attributed to the electrical relaxation processes. Further, it is also observed that the pure sample has the highest dielectric constant values than the bismuth doped yttrium oxide samples. It may due to the introduction of holes in the host yttrium oxide. At the same time, increasing order of dielectric constant on higher doping concentration of bismuth shows the improved surface transport properties suitable for a dielectric gate material.

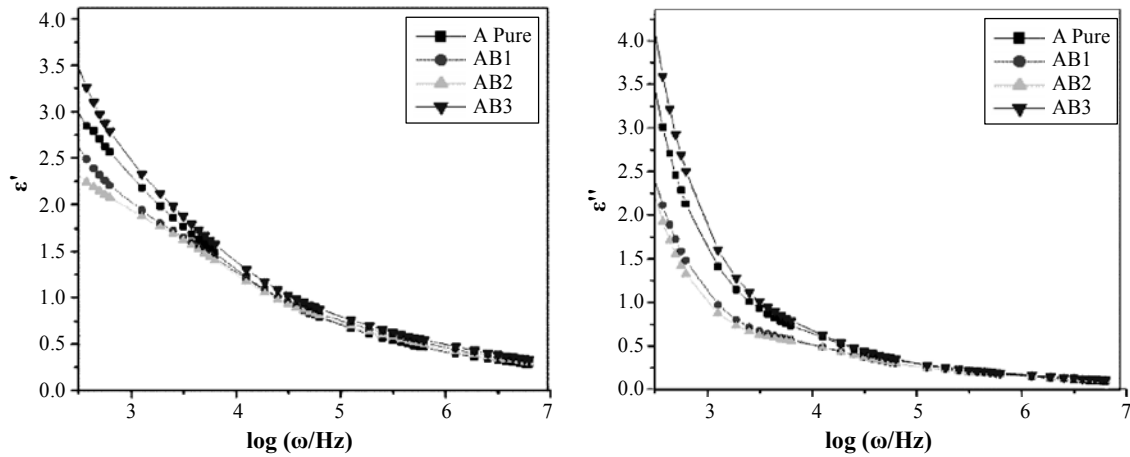


**Fig. 4: Variation of dielectric constant and loss factor of pure yttrium oxide and bismuth doped  $\text{Y}_2\text{O}_3$  at room temperature**

Fig. 5 shows the variation of tangent loss with frequency of pure yttrium oxide and bismuth doped yttrium oxide samples at different dopant concentration prepared by sol-gel method. The tangent loss spectra of all these samples are characterized by peaks appearing at characteristic frequency for different doping concentration suggesting the presence of relaxing dipoles in all the samples. The strength and frequency of relaxation depends on the characteristic property of dipolar relaxation.

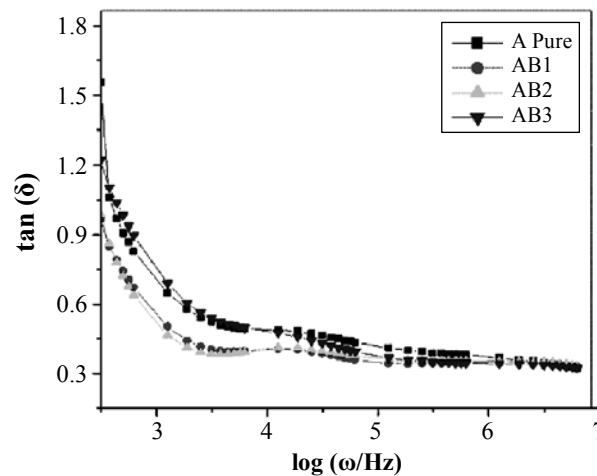


**Fig. 5: Variation of dielectric loss factor with frequency at room temperature of pure yttrium oxide and bismuth doped yttrium oxide**

## CONCLUSION

In this paper, structural and electrical properties of pure and bismuth doped yttrium oxide samples prepared by sol-gel method of various doping concentration are analysed. FTIR studies confirm the presence of elements. It was observed from the XRD analysis that the doping increases crystallinity nature and also the crystallinity increases with doping concentration. The maximum conductivity achieved was in the order of  $3.5 \times 10^{-7} \text{ Scm}^{-1}$  for pure sample. It can also be seen that dielectric loss decreases with the increase in dopant concentration and become very low value at high frequency region.

## REFERENCES

1. Y. M. Wu and J. T. Lo, Jap. J. Appl. Phys., **37**, 5645 (1998).
2. A. F. Andreeva, A. G. Sisonyuk and E. G. Himich, Phys. Stat. Solidi A, **145**, 441 (1994).
3. W. R. Manning, Jr O. Hunter and Jr B. R. Powell, J. Am. Cer. Soc., **52**, 436 (1969).
4. C. H. Ling, J. Bhaskaran, W. K. Choi and L. K. Ah, J. Appl. Phys., **77**, 6350 (1999).
5. M. H. Cho, D. H. Ko, K. Jeong, S. W. Whangbo, C. N. Whang, S. C. Choi and S. J. Cho, Thin Solid Films, **349**, 266 (1999).
6. F. Jollet, C. Noguera, N. Thromat, M. Gautier and J. P. Duraud, Phys. Rev. B, **42**, 7587 (1990).
7. F. Jollet, C. Noguera, M. Gautier, N. Thromat and J. P. Duraud, 991, Influence of Oxygen Vacancies on the Electronic Structure of Yttrium Oxide, J. Am. Cer. Soc., **74**, 358 (1991).
8. D. R. Mueller, D. L. Ederer, J. van Ek, W. L. O'Brien, Q. Y. Dong, J. J. Jia and T. A. Callcott, Phys. Rev. B, **54**, 15034 (1996).
9. Y. N. Xu, Z. Q. Gu and W. Y Ching, Phys. Rev. B, **56**, 14993 (1997).
10. R. Subramanian, P. Shankar, S. Kavithaa, S. S. Ramakrishnan, P. C. Angelo and H. Venkataraman, Mat. Lett., **48**, 342 (2001).
11. S. Xiaoyi and Z. Yuchun, Rare Metals, **30**, 33 (2011).
12. M. K. Shobana and S. Sankar, J. Mag. Mag. Mat., **321**, 3132 (2009).
13. Y. Liu, Z. F. Zhang, B. King, J. Halloran and R. M. Laine, J. Am. Cer. Soc., **79**, 385 (1996).

14. V. Fruth, A. Ianculescu and G. Voicu, *J. Euro. Cer. Soc.*, **26**, 3011 (2006).
15. C. Suryanarayanan and M. G. Norton, 'X-ray Diffraction, A Practical Approach, Plenum Press, New York (1998).
16. B. A. Boukamp, *Sol. Sta. Ionics*, **20**, 31 (1986).
17. B. A. Boukamp, *Sol. Sta. Ionics*, **18 & 19**, 136 (1986).
18. D. K. Pradhan, R. N. P. Choudhary and B. K. Samantaray, *Int. J. Elec. Sci.*, **3**, 597 (2008).

*Accepted : 16.03.2016*